Glycoconj J (2015) 32:345–359
DOI 10.1007/s10719-015-9592-8

ORIGINAL ARTICLE

Evolutionary diversity of social amoebae N-glycomes may support interspecific autonomy

Christa L. Feasley[1,3] · Hanke van der Wel[1] · Christopher M. West[1,2]

Received: 23 December 2014 / Revised: 11 April 2015 / Accepted: 14 April 2015 / Published online: 19 May 2015

Abstract Multiple species of cellular slime mold (CSM) amoebae share overlapping subterranean environments near the soil surface. Despite similar life-styles, individual species form independent starvation-induced fruiting bodies whose spores can renew the life cycle. N-glycans associated with the cell surface glycocalyx have been predicted to contribute to interspecific avoidance, resistance to pathogens, and prey preference. N-glycans from five CSM species that diverged 300–600 million years ago and whose genomes have been sequenced were fractionated into neutral and acidic pools and profiled by MALDI-TOF-MS. Glycan structure models were refined using linkage specific antibodies, exoglycosidase digestions, MALDI-MS/MS, and chromatographic studies. Amoebae of the type species *Dictyostelium discoideum* express modestly trimmed high mannose N-glycans variably modified with core α3-linked Fuc and peripherally decorated with 0–2 residues each of β-GlcNAc, Fuc, methylphosphate and/or sulfate, as reported previously. Comparative analyses of *D. purpureum, D. fasciculatum, Polysphondylium pallidum,* and *Actyostelium subglobosum* revealed that each displays a distinctive spectrum of high-mannose species with quantitative variations in the extent of these modifications, and qualitative differences including retention of Glc, mannose methylation, and absence of a peripheral GlcNAc, fucosylation, or sulfation. Starvation-induced development modifies the pattern in all species but, except for universally observed increased mannose-trimming, the N-glycans do not converge to a common profile. Correlations with glycogene repertoires will enable future reverse genetic studies to eliminate N-glycomic differences to test their functions in interspecific relations and pathogen evasion.

Keywords Social amoebae · Cellular slime molds · *Dictyostelium* · Evolution · N-glycan

Electronic supplementary material The online version of this article (doi:10.1007/s10719-015-9592-8) contains supplementary material, which is available to authorized users.

✉ Christopher M. West
westcm@uga.edu; Cwest2@ouhsc.edu

Christa L. Feasley
christa.feasley@thermofisher.com

[1] Department of Biochemistry & Molecular Biology, Oklahoma Center for Medical Glycobiology, University of Oklahoma Health Sciences Center, 975 NE 10th St., BRC-415, OUHSC, Oklahoma City, OK 73104, USA

[2] Department of Biochemistry and MolecularBiology, Fred C. Davison Life Sciences Complex, The University of Georgia, Athens, GA 30602, USA

[3] Present address: Thermo-Fisher Scientific, West Palm Beach, FL 33407, USA

Abbreviations

2-AB	2-aminobenzamide
ACN	Acetonitrile
CSM	Cellular slime mold
DTT	Dithiothreitol
H8N4F	Notation for a glycan containing 8 hexoses, 4 HexNAc residues, and 1 deoxyHex expected to be fucose
TFA	Trifluoroacetic acid

Introduction

Dictyostelium discoideum (*Dd*) is a social amoeba, also known as a cellular slime mold (CSM), that resides in soils around the world. Kin to other amoebae such as *Acanthamoeba* and *Entamoeba*, the group diverged from other major eukaryotic

lineages during the crown radiation [1–3]. The social amoebae consist of over a hundred species that can cohabitate the same soil environment where they feed phagocytically on bacteria and yeasts. In response to starvation, cells chemotactically aggregate to form multicellular structures termed slugs, which migrate to the soil surface and culminate to form fruiting bodies, whose spores can then be dispersed to new environments [1]. The up to 100,000 cells of the slug are specialized into prespore and multiple prestalk cell types, which differentially contribute to the formation of spores and the supporting stalk. Individual species modify this basic developmental program in characteristic ways.

The unicellular amoebae are enveloped by an extensive glycocalyx [4] with a high content of high-mannose N-glycans. Classical studies documented that *Dd* glycans derive from the canonical $Glc_3Man_9GlcNAc_2$-PP-Dol precursor, and consist of a family of $Man_{6–9}$ structures variably modified by bisecting and intersecting β4-GlcNAc residues, core α3-linked fucose (Fuc), and peripheral Man-linked Fuc, SO_4 and CH_3-PO_4 [5], as recently confirmed by mass spectrometry (MS) studies [6–8]. During development, these structures undergo major changes in terms of the number of substituents and extent of Man-trimming [5, 9]. The major question we address here is whether discrete structures support growth and developmental processes universal to the CSMs, or processes specific to individual species.

Despite physical proximity in the soil, the various species develop independently [*e.g.*, 10, 11] and the glycocalyx may contribute to their mutual avoidance. N-glycans have been implicated in amoeba-bacteria interactions [12], and multiple glycosyl modifications appear to influence cell interactions during growth and development. For example, a global fucosylation mutant exhibits slow growth and forms abnormal cell aggregates in suspension [13], mucin-type O-glycosylation mutants exhibit abnormal sorting of prespore and prestalk cells [14] and abnormal spore coat assembly [15, 16], anionic N-glycan processing mutants exhibit altered kinetics of protein compartmentalization [17, 18], and cytoplasmic glycosylation mutants exhibit abnormal O_2-sensing [19, 20]. Studies from our laboratory and others have begun to use MS to explore the N-glycomes of two cellular slime molds [3, 6–8, 21, 22] used as model organisms for interspecific relations, *Dd* and *Dictyostelium purpureum* (*Dp*). Recently, the genomes of additional social amoebae have been sequenced [2, 23], opening the door to apply genomics to glycogene identification to enable a genetic approach to addressing these questions. Their phylogeny, which spans the diversity of known CSMs [24], is represented in Fig. 1a.

In this study we compared the N-glycomes of five anciently diverged CSM species during vegetative growth and upon starvation induced development. Though all CSM N-glycans appear to derive from the same $Glc_3Man_9GlcNAc_2$ precursor, their glycomic profiles as revealed by MALDI-TOF-MS are highly distinctive and do not converge during development. Based on a recent analysis of the prominent cell surface glycoprotein gp130 [6], this repertoire is likely to be reflective of cell surface glycocalyx differences that have the potential to influence interspecific and kin recognition, predator–prey relationships, and commensal interactions with other bacteria.

Experimental procedures

Cell strains and cell culturing

Dictyostelium purpureum (*Dp*) strain *Dp*-1 was from Adam Kuspa (Baylor College of Medicine). *Dictyostelium discoideum* (*Dd*) strain Ax3, *D. fasciculatum* (*Df*), *Polysphondylium pallidum* (*Pp*), and *Acytostelium subglobosum* (*As*) were from the *Dictyostelium* Stock Center (Northwestern University). Amoebae were grown on SM (or SM/5 for *As*) agar plates in association with *Klebsiella aerogenes* (*Ka*) bacteria at 22 °C using standard methods [25]. Growth stage amoebae were harvested as they began to clear the *Ka* lawn (48–60 h). Cells were scraped off and suspended into by vortexing or pipetting into ice-cold 50 mL KP buffer (10 mM potassium phosphate, pH 6.5), pelleted by repeated centrifugation/resuspension at 1000×*g* for 1 min until cleared of bacteria, and counted in a hemacytometer. Aliquots of 1×10^7 cells were transferred to 1.5-mL microcentrifuge tubes, pelleted again, and snap-frozen at −80 °C. For development, the washed cells were resuspended at 2×10^8 cells/mL in KP buffer, and 0.6 mL was spread on a 10-cm diameter non-nutrient agar plate as described [25] and incubated under fluorescent room lighting at 22 °C. At the slug stage (~12–18 h), cells were scraped, spun into the bottom of a 1.5-mL tube, and frozen as above.

N-glycan release and recovery

Cell pellets (1×10^7 cells) were lysed by probe sonication in 200 μL 5 % formic acid, and sequentially digested with pepsin and PNGase A as described [21]. Alternatively, cell pellets were resuspended in 200 μL 6 M urea in 25 mM ammonium bicarbonate (pH 7.8) with probe sonication, reduced and alkylated, diluted, and sequentially digested with trypsin and PNGase F or Endo-H_f as described [21]. To recover N-glycans, samples were diluted with an equal volume of 0.1 % (*v*/*v*) TFA in water and applied to a pre-equilibrated C_{18}-SepPak (100 mg) cartridge (Waters). Glycans were purified from the flow-through fraction by absorption to and release from a Carbograph cartridge, with 0.1 % TFA in 50 % ACN, and dried in a vacuum centrifuge, as described [21]. To enrich for H10N2-H12N2 N-glycans from Dp, samples were fractionated on a porous graphitized carbon (PGC) column (Hypercarb, 2.1×100 cm, ThermoFisher) eluted with an increasing ACN gradient (5–45 % over 60 min). Fractions were surveyed for glycan content by MALDI-TOF-MS.

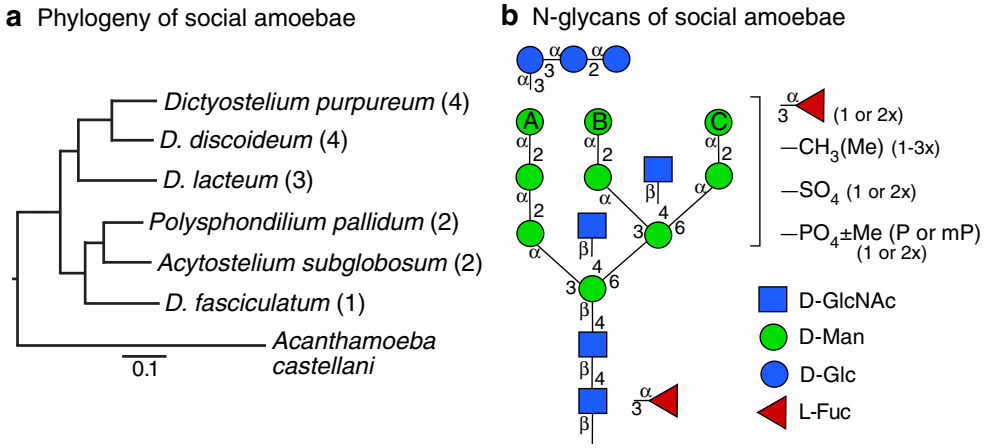

Fig. 1 Phylogeny and N-glycans of social amoebae. **a**. The social amoebae are classified into 4 groups denoted in parentheses) based on the phylogeny of a core group of housekeeping genes (adapted from Romeralo *et al.* [24]). The last common ancestors of these groups date back 300–550 million years. All but the group 3 species *D. lacteum* are examined in this study. **b**. The N-glycan precursor of *D. discoideum* corresponds to the $Glc_3Man_9GlcNAc_2$ structure found in most eukaryotes, and is typically immediately processed by α-glucosidases I and II to the $Man_9GlcNAc_2$ structure shown. This is further processed by α-mannosidase mediated removal of peripheral Man residues, and addition of peripheral substituents and core α3-linked Fuc as indicated. Arms are denoted as A, B or C as indicated

Enrichment of anionic glycans

The Carbograph-purified N-glycans were resuspended in 100 μL 5 mM Trizma base (pH 9.6) and anionic glycans enriched by adsorption to QAE-Sephadex A-50 (Sigma-Aldrich) and NaCl-elution, as previously described [21], and desalted on a Carbograph cartridge. The flow-through fraction was recovered as an enriched fraction of neutral glycans.

Glycan derivatizations

Spin column permethylation using methyl iodide (CH_3I, d_0-PerM) or deuterated methyl iodide (CD_3I, d_3-PerM) was performed as described [21, 26]. Alternatively, N-glycans were labeled with 2-aminobenzamide (2-AB), purified by Whatman 3MM paper chromatography, and eluted with 100 μL 5 % acetic acid in H_2O, as previously described [6, 21].

MALDI-TOF-MS analysis

N-glycan samples (native, 2-AB labeled, or permethylated) were dried and resuspended in 20 μL of 50 % ACN/H_2O. 0.5 μL was spotted onto polished steel MALDI target plate with an equal volume 20 mg/mL 2,5-dihydroxybenzoic acid in 50 % (*v*/*v*) ACN/H_2O and vacuum dried for co-crystallization. For glycan fragmentation, TOF–TOF MS/MS experiments were performed by accelerating fragment ions generated by laser-induced dissociation at 19 kV using Ar as the collision gas in the LIFT™ device incorporated in the Bruker Ultraflex II MALDI-TOF-TOF (Bruker Daltonics, Billerica, MA) instrument used for these studies [21, 27]. Spectra were analyzed in GlycoWorkbench [28].

Exoglycosidase digestion

α-mannosidase 2-AB labeled N-glycans, or native N-glycans enriched in H10N2-H12N2 species, were treated with purified [21] jack bean α-mannosidase (Sigma-Aldrich), as described previously [6].

α-glucosidase-I Glycans from 2×10^7 *Dp* cells prepared by the pepsin/PNGase A method (see above) were resuspended into 50 μL 10 mM NH_4Ac, pH 6.8. An aliquot of N-glycans (3 μL) was digested with 1 μL (activity = 0.2 nmol/μL-min at 37 °C) yeast processing α-glucosidase-I [29, 30] (a generous gift from Dr. C. Scaman, University of British Columbia) previously microdialyzed against 10 mM NH_4Ac for 2 h at 4 °C. To confirm activity under these conditions, 1 μL of 1 mM Glcα1,2Glcα1,3Glcα-O-CH_3 (gift of Dr. Scaman) was added to 2.5 μL of enzyme. α-glucosidase-I digests were incubated at 37 °C for 1–18 h before analysis by MALDI-TOF MS.

SDS-PAGE analysis and Western blotting

Cell extracts (25 μg total protein) were electrophoresed on an SDS-PAGE gel (NuPAGE, Invitrogen), blotted onto 0.45-μm pore size nitrocellulose (BioRad) and probed with a core α3-linked fucose specific antibody as described [6, 21].

Quantification of glycan species

N-glycan types were quantitated from positive ion mode MALDI-TOF-MS data of permethylated glycans, by dividing the ion current from the monoisotopic peak of each species type by the sum of monoisotopic peak values of all detected N-glycans in the sample.

Database searches

Gene homologs were searched for using the BLASTP algorithm seeded with *Dd* [31] and *Dp* [3] glycogene sequences. CSM genomes were searched at http://dictybase.org/ (*Dd*, *Dp*), http://sacgb.fli-leibniz.de (*Df* and *Pp*), and http://acytodb.biol.tsukuba.ac.jp/cgi-bin/index.cgi?org=as [*Database Release 2.0(2010/2/23)*] (*As*).

Results

Neutral N-glycomes

The main features of N-glycans of the type species *Dd* are illustrated in Fig. 1b. These structures are derived from the typical, highly-conserved, eukaryotic $Glc_3Man_9GlcNAc_2$ lipid-linked oligosaccharide precursor followed by post-transfer Glc-removal [5, 7]. For the present study, cells were solubilized in formic acid, to inhibit endogenous endo-H like activity, and sequentially digested with pepsin and peptide:N-glycosidase A (PNGase A), to allow release of core α3-fucosylated structures. N-glycans were purified on a Carbograph cartridge, and analyzed natively or after permethylation or derivatization with 2-AB at the reducing terminus. As shown in Fig. 2a, analysis of underivatized (native) glycans from bacterially-grown cells of the *Dd* laboratory strain Ax3 by MALDI-TOF-MS revealed diverse neutral high-mannose glycans predominantly consisting of Man_5 to Man_9 species, variably decorated with 1–2 GlcNAc residues (in addition to the core GlcNAc2) and up to one Fuc. Similar compositions were observed when comparing native and derivatized glycans (supplemental Fig. S1). Previous chromatographic studies [8] suggested that initial Man-trimming to generate the Man8 species occurs on the A- rather than the more common B-arm site (Fig. 1b). Where present, the third and fourth GlcNAc residues are β4-linked at the intersecting and bisecting positions, based on prior exoglycosidase, NMR and MS/MS studies [6, 7, 32]. The Fuc is typically α3-linked to the core GlcNAc [5–7] based on resistance to digestion to PNGaseF, MS/MS studies, and epitope analysis with anti-HRP. Anionic glycans are minimally detectable by positive ion mode MS, and are examined separately below.

Mannose trimming

A similar analysis of total N-glycans from bacterially-grown, growth stage *Dp*, *Df*, *Pp* and *As* cells showed that each expresses predominantly H5 to H9 structures as for *Dd* (Fig. 2b–e). Since these species also possess the genetic complement to encode the enzymes that assemble the archetypal $Glc_3Man_9GlcNAc_2$-lipid-linked oligosaccharide donor (not shown), it is likely that these structures derive from Glc and Man trimming after transfer to the protein acceptor. In general, the hexose residues were confirmed to consist of α-linked Man residues based on sensitivity to removal by the broad spectrum α-mannosidase from jack beans (Fig. S2, Fig. 4b for *Dp*). Individual α-mannosidase resistant glycans, and anionic glycans (*) which are insensitively detected in positive ion mode analysis of unfractionated material, are examined further in later sections below. Interestingly, each species displays a characteristic profile indicating stereotyped variations in the average extent of Man-trimming, as shown in Figs. 2 and S2 for native glycans and summarized below in Fig. 8a for permethylated glycans. Specifically, Man_6 species are more abundant than the other processed states observed, including Man_5, Man_7, Man_8 and Man_9 in *As*. Likewise, Man_7 is the most abundant in *Dp* and *Df*, and Man_8 is the most abundant in *Dd* and *Pp*. Further studies are needed to establish which Man residues are trimmed and the extent of heterogeneity, which cannot be ascertained by MALDI-TOF-MS experiments. As described below, these high-mannose structures were variably modified with neutral and anionic substituents, the quality and degree of which also exhibited substantial species specificity. Only H9N2 structures tended to be less modified.

Peripheral GlcNAc

A substantial fraction of growth stage *Dd* N-glycans were modified with an additional HexNAc residue (Fig. 2a), shown previously [33] to represent GlcNAc in β4-linkage to the α6-linked Man (intersecting position), or with 2 HexNAcs the second of which is β4-linked to the βMan (bisecting). N-glycans with 3 HexNAcs (including the chitobiose core) were predominant in *Df*, *Pp* and *As* (Fig. 2c–e). Under the conditions of treatment with endoglycosidase Hf employed here, the N3 N-glycans of the other species are, like the N3 and N4 glycans of *Dd*, resistant to release (Fig. S3). MS/MS results were most consistent with an intersecting position on the α6-linked Man, owing to detection of a MeHex3HexNAc fragment ion (*m*/*z* 723.5) and failure to detect ions diagnostic for alternative positions (*Pp*; Fig. 6, below). Whereas peripheral GlcNAc residues were found on all *Dd* Man-processing variants except Man9, in *As* peripheral HexNAc favored the H6 species over the also abundant H7 and H8 isoforms. The abundant H7 and H8 species present in *Df* and *Pp*, respectively, were efficiently modified by peripheral HexNAc. Thus this HexNAc is unlikely to be related to the β2-linked GlcNAc installed on Manα1-3Manβ1– by GlcNAc-T1 (MGAT1) as the initial step in processing to complex forms of animals. HexNAc3 (N3) species were of low abundance in *Dp*, but were more common in our previous analysis of *Dp* [3]. The reason for this discrepancy is not clear but might related to the use of CHAPS rather than formic acid extracted material. Ions

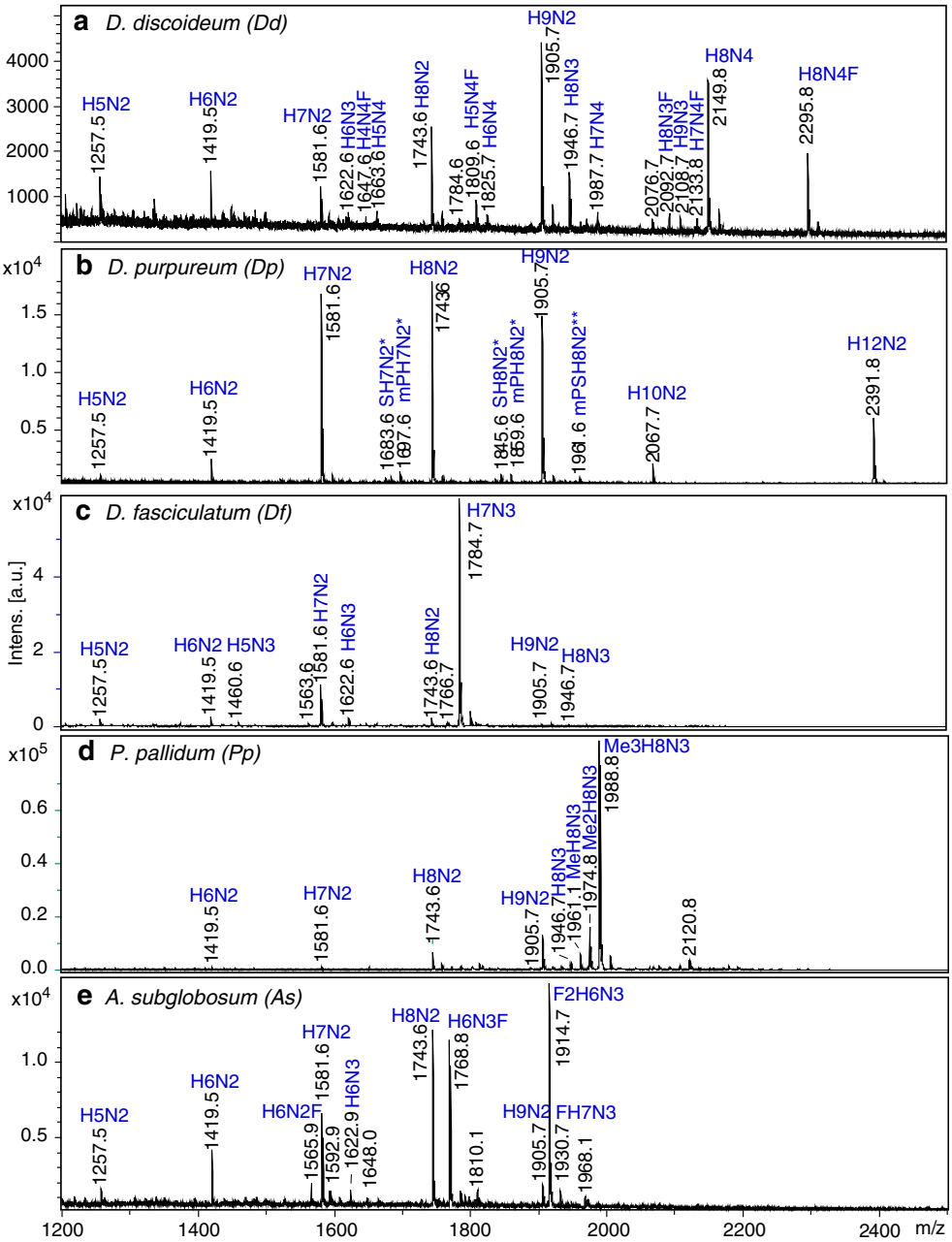

Fig. 2 Neutral growth stage N-glycan glycomes are species-specific. N-glycans were released from pepsin-digested whole cell extracts of bacterially grown cells, using PNGase A, and profiled by MALDI-TOF-MS in positive ion mode. Most ions were observed as $[M+Na]^+$ accompanied by minor $[M+K]^+$ (+16) ions. Anionic species were detected as $[M–H+2Na]^+$ (*) or $[M–2H+3Na]^+$ (**). Representative spectra from the 5 species are shown in panels **a**-**e**. Compositions are noted by H=Hex, N=HexNAc, and F=Fuc. Except as noted, Hex=Man and HexNAc=GlcNAc, according to previous composition analyses, and exoglycosidase digestions (Fig. S2). Position of F at the right end of the string indicates that MS-MS fragmentation located its linkage at the core GlcNAc. Spectra are representative of at least 2 independent biological replicates

corresponding to the presence of a fourth HexNAc as found in *Dd* were not detected in the other species. Though the simplest assumption is that the third HexNAc in *Dp*, *Df*, *Pp* and *As* represents an intersecting β-GlcNAc, the possibility of a bisecting position or some other configuration or HexNAc type, cannot be excluded.

Fucosylation

N-glycans of *Dd* are frequently substituted with α3-linked Fuc residues on the reducing terminal (Asn-linked) GlcNAc [6, 7, 34], as also observed in plants and invertebrates. This structure is recognized as an epitope by anti-HRP antibody and, based on Western blotting, was similarly if not more abundant in growth stage *As* (Fig. 3a). The occurrence of this linkage in *As* was supported by the detection by MS of multiple singly and doubly fucosylated species after digestion with PNGase A (Fig. 2e) but not PNGase F (data not shown), which cleaves core α6- but not α3-fucosylated structures [7]. Core α3-fucosylation was highly enriched on N-glycans with one or two peripheral HexNAc residues in *Dd* and *As*, suggesting an interdependence of the GTs that mediate the addition of their respective sugars. Whereas a range of Man-trimmed *Dd* glycans were core α3-fucosylated, this modification was preferentially enriched on Man_6 species in *As*.

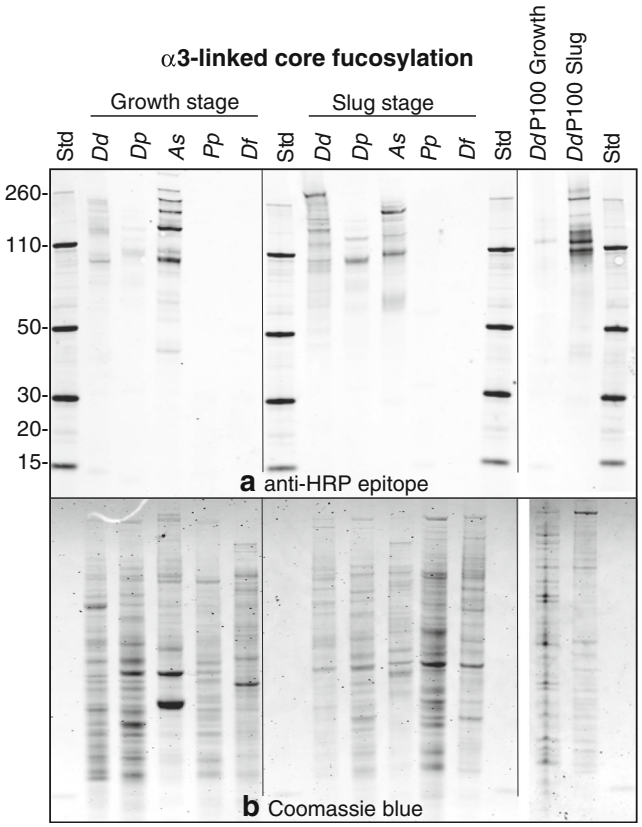

Fig. 3 Core α3-fucosylation of amoeba glycoproteins. **a**. Whole cell CSM extracts (growth or slug stage as indicated) were Western-blotted and probed with affinity-purified rabbit anti-HRP Ab. The *Dd* membrane (P100) panels at the right confirm previously reported [7] developmental regulation of the core α3-Fuc epitope. M_r values ($\times 10^3$) are shown for the protein standards at the upper left. **b**. A parallel gel was stained with Coomassie blue as a loading control

Core α3-fucosylation was also implicated in growth-stage *Dp* cells by anti-HRP Western blotting (Fig. 3a), but fucosylated N-glycans were not observed by MS (Figs. 2b and 8e) [3]. However, core α3-fucosylated structures were found by MALDI-TOF-MS in slug-stage *Dp* cells (see below), which correlated with increased anti-HRP labeling in Western blots (Fig. 3), so low level core α3-fucosylation probably occurs in growing *Dp* cells too. A low level of deoxyHex (possibly Fuc) was observed in permethylated *Pp* N-glycans, but no evidence for fucosylation was found in *Df* (Figs. 3, 8e).

At the protein level, the Western blot analyses showed little evidence for M_r conservation of the carriers of core Fuc modifications, either at different developmental stages within the same species, or between species (Fig. 3), suggesting that the proteins that these glycans modify are evolutionarily divergent. The M_r profiles of anti-HRP reactive bands in total cell and total membrane fractions were distinctive, suggesting that a large fraction of α3-core fucosylated glycoproteins reside in a non-membranous pool (Fig. 3).

As also expressed glycans with multiple deoxyHex residues, assumed to represent Fuc based on analogy with *Dd* [6]. Peripheral fucosylation was not observed in the absence of core fucosylation, suggesting a dependence of peripheral FTs on the core α3-FucT, which remains to be identified.

Although core α6-fucosylation has been reported in *Dd* [34, 35], no evidence for Fuc or other deoxyHex residues was obtained in the present analysis of bulk PNGase F-released N-glycans from any of the species. If present, core α6-Fuc is a minor substitution, or occurs in combination with another modification that interferes with cleavage by PNGaseF.

H12N2 species from Dp is glucose-capped

Dp uniquely accumulated substantial levels of H10N2 and H12N2 structures (Figs. 2b and 4c), which could be released by Endo Hf (Fig. S3b). To examine the identity of the additional Hex residues, native glycans samples from slug cells were treated with jack bean α-mannosidase which is capable of removing all α-linked Man residues. After enrichment of non-fucosylated N-glycans on a porous graphitized column, N-glycans with 4–7 hexoses (H(4–7)N2) were degraded to H(1–3)N2, indicating successful removal of almost all Hex residues (Fig. 4a, b). In comparison, the H12N2 and H11N2 species were converted to H(10–8)N2 species, which could be explained by protection of the A-arm by 3 Glc residues (7 Hex residues total, see Fig. 1b) derived from the $Glc_3Man_9GlcNAc_2$-LLO precursor. The presence of a Glc cap was confirmed by α-glucosidase I digestion of a pool of growth stage *Dp* N-glycans, which trims only the terminal α2-linked Glc from the $Glc_3Man_9GlcNAc_2$ precursor. As shown in Figs. 4c and d, a single Hex residue was removed from only the H12N2, and the H12N3 species observed in this trial, suggesting that *Dp* incompletely processes its initial N-glycans. The presence of the third HexNAc in the H12N3 species, though only variably observed (compare Fig. S4a), confirms that these glucosylated glycans did not artifactually derive from contaminating lipid-linked precursor, and in turn indicates that peripheral HexNAc addition (see above) does not depend on N-glycan processing, as shown before for the intersecting β4-GlcNAc [8]. The disappearance of species smaller than H8N2 after α-mannosidase digestion indicates that deglucosylation precedes Man-processing for most N-glycans.

Peripheral mannose methylation in Pp

The most abundant N-glycan of growing *Pp* was consistent with a trimethylated (+42) H8N3 species, which was accompanied by lesser quantities of ions corresponding to dimethylated, monomethylated and nonmethylated forms (Figs. 2d and 5a). Only an H8N3 species was detected after permethylation (Fig. 5b), indicating that the mass increment was due to Me groups substituted on sugar -OH groups. This

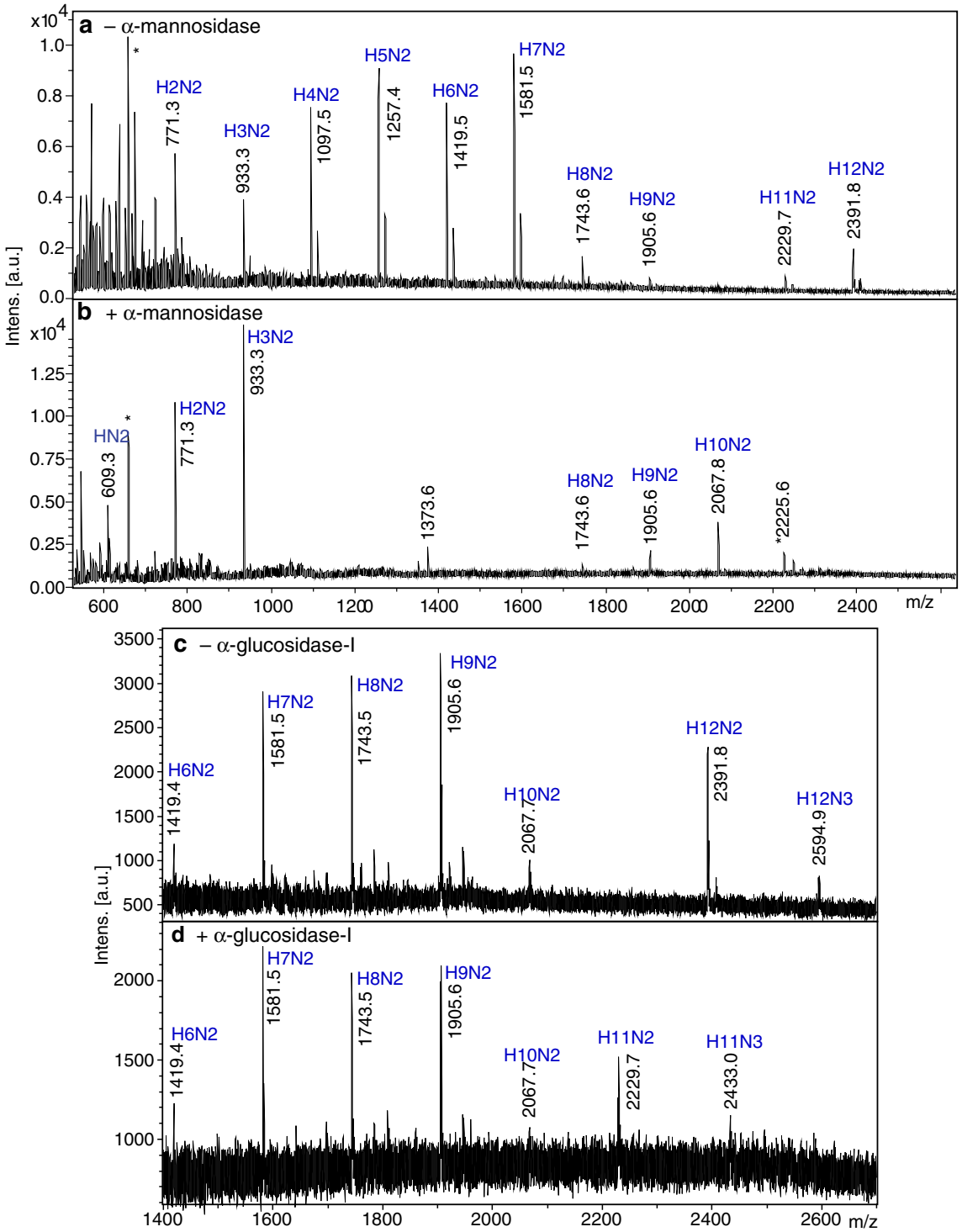

Fig. 4 *Dp* N-glycans are high-mannose and partially retain Glc3 caps. N-glycans were released from *Dp* slugs (**a, b**) or growth stage (**c, d**) cells with PNGase A. Non-fucosylated species were enriched on a porous graphite column (**a, b**). Samples were subjected to MALDI-TOF-MS in positive ion mode before (**a**) or after (**b**) digestion with non-specific jack bean α-mannosidase, or yeast α-glucosidase-I (**c, d**). *A*sterisks indicate a matrix or α-mannosidase background peak

was investigated further by perdeuteration, which yielded an *m/z* value that was 9 less than expected (*m/z* 2533 compared to 2542) for a fully perdeuterated derivative (Fig. 5c), confirming the initial presence of 3 CH_3 (Me) groups which would each contribute a mass of 14 rather than the 17 of CD_3. In MS/MS analysis of the abundant trimethylated native glycan, the absence of MeH fragment ions and presence of MeH2 (Fig. 5d) is most consistent with the occurrence of mono-

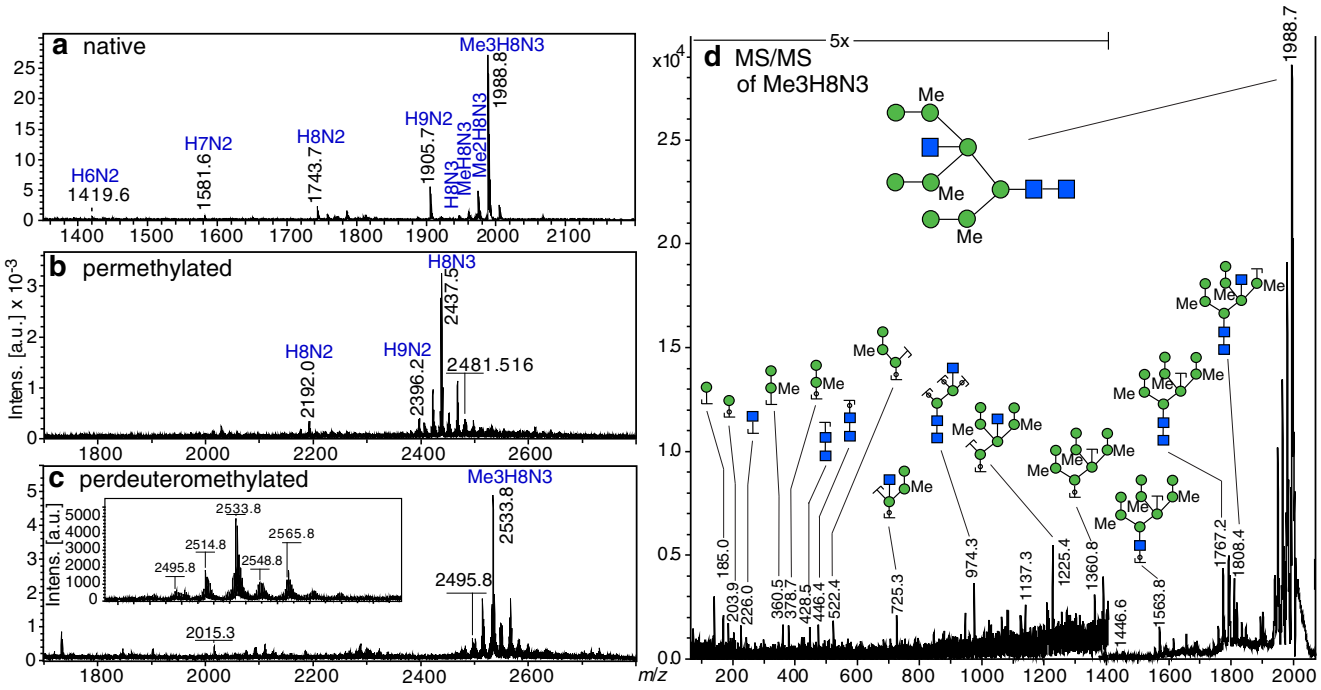

Fig. 5 Methylated N-glycans of *Pp*. **a.** MALDI-TOF-MS analysis of N-glycans from growth stage *Pp* suggested that the most abundant species was H8N3 modified by 3 Me (CH_3) groups. **b**. Permethylation with methyl iodide (CH_3I) eliminated the mass increment of the CH_3 groups, indicative of occurrence on sugar hydroxyls. **c**. Perdeuteration with CD_3I confirmed the expected mass difference due to prior native methylation. *Inset*: the low abundance ions surrounding the central Me3H8N3 ion in **b** and **c** do not correspond to partially methylated derivatives ($m/z = \Delta 42$). **d.** MS/MS of Me3H8N3 from *Pp*. MALDI-TOF-TOF-MS of *Pp* glycan ion m/z 1988 (panel a), assigned as $Me_3Man_8GlcNAc_3$. Ions are $[M+Na^+]^+$ forms. The predicted configuration of the parent ion is shown. Potential interpretations of fragment ions induced by CID, as assigned in GlycoWorkbench, are illustrated. b- and z-type fragment ions are denoted with a half bracket; c- and y-ion fragments are depicted with an 'o' at the fragmentation site

methylation of subterminal Man residues, one on each arm. The tri-methylated N-glycan was resistant to α-mannosidase digestion (Fig. S2d), indicating that each arm was modified and that methylation of the underlying Man residue interferes with enzymatic release. Further studies will be required to determine the position(s) of Me-linkage to the Man residues. No evidence for methylation was found in the other CSM species.

Developmental changes in neutral N-glycomes

The total neutral N-glycan pool from the slug stage of *Dd* consisted of a range of high mannose structures related to those of growth state cells except for the smaller average number of Man residues (Fig. 6a), in agreement with prior work documenting increased Man-trimming during development [7, 9, 33, 36]. Each of the other the CSM species exhibited a similar trend, although *Pp* maintained H8 as the predominant species which may be due to protection by continued Man-trimethylation (Fig. 6d). Modestly decreased peripheral HexNAc was observed in *Dd*, *Pp* and *As*, whereas *Df* and *Dp* remained similar. *Dd* and *Dp* showed increased fucosylation in the slug stage (Fig. 6a, b). This was consistent with modestly increased reactivity with the anti-HRP antibody (Fig. 3), suggesting that at least some of these residues are core α3-linked. Some slug *Pp* glycans contained up to 3 Fuc residues whose positions remain to be mapped. By contrast, *As* N-glycans exhibited the opposite trend of less fucosylation in slugs (Fig. 6e). *Dd* and *Pp*, but not *Dp*, preferentially fucosylated glycans with peripheral HexNAc residues.

Anionic glycans

Sulfation and methylphosphorylation are prominent peripheral modifications of *Dd* N-glycans, but require negative ion mode MS, enrichment, and/or permethylation for efficient detection. To investigate their occurrence in other species, native anionic glycans were enriched from growth stage cells by a QAE-Sephadex anion exchange method [21], and displayed in negative (Fig. 7, left panels) or positive ion mode (Fig. S4). Neutral glycans only were detected in the QAE-flow through fractions (not shown and Fig. S4a). Elution with 70 mM NaCl yielded, after desalting, a variety of ions the great majority of which could be assigned as N-glycans modified by methyl phosphate, sulfate or both. Negative ion mode analysis was generally more sensitive than positive ion mode analysis (compare Fig. 7 with Fig. S4b), but the latter helped to confirm assignments of the major ions because they generally occurred

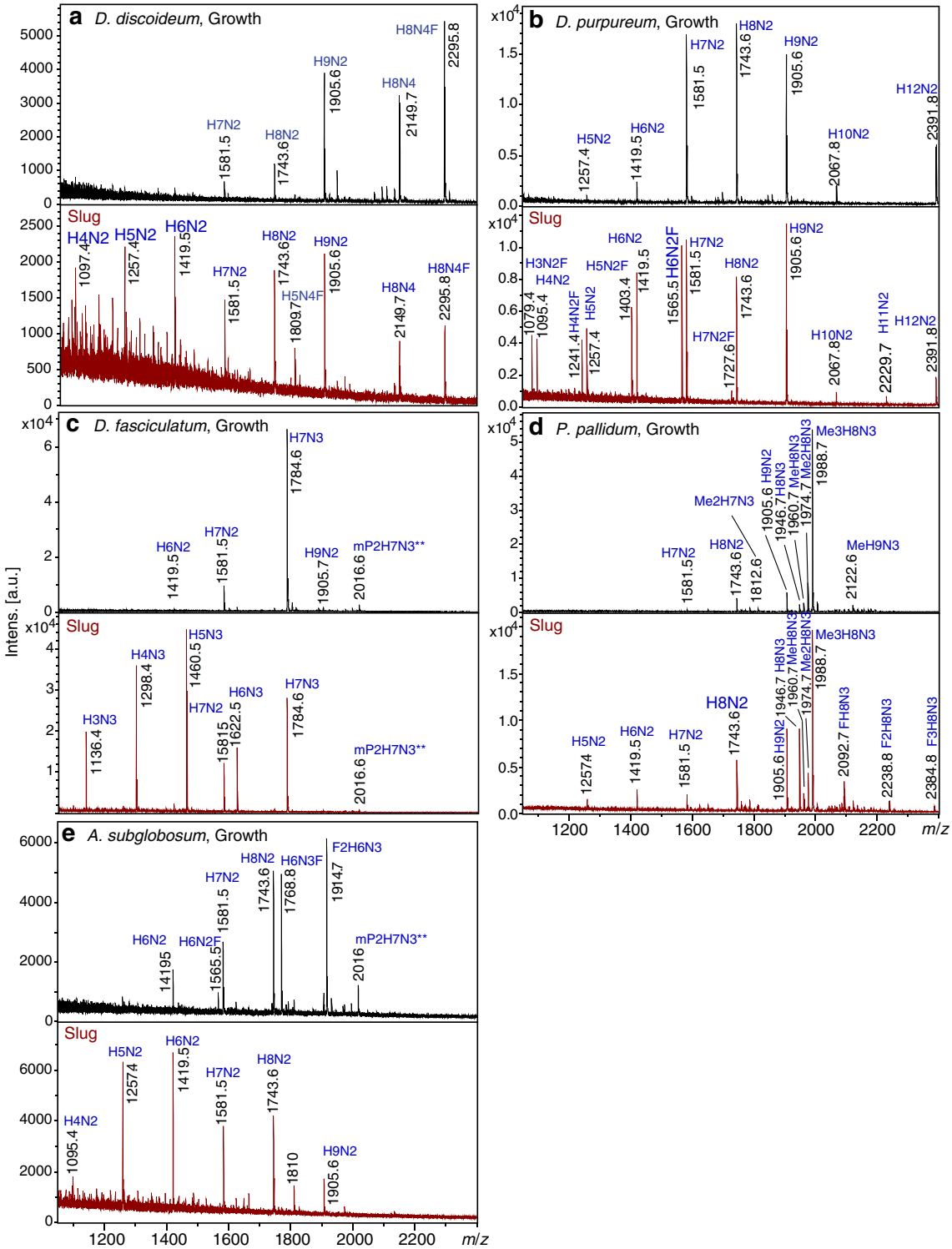

Fig. 6 Developmental regulation of N-glycan expression. N-glycans prepared from slug stage cells of each of the 5 species (**a-e**) were profiled in positive ion mode as in Fig. 2. Corresponding growth stage samples (bacterially grown biological replicates of samples in Fig. 2), are shown for comparison. No ions were detected above *m/z* 2400. Assignments are based on additional permethylation spectra and MS/MS analysis where possible. Ions are $[M+Na]^+$, except *=$[M–H+2Na]^+$, or **=$[M–2H+3Na]^+$

as singly-charged disodiated or trisodiated species (with compensatory deprotonation) for mono-anionic and di-anionic glycans, as opposed to the singly-charged deprotonated or di-deprotonated/monosodiated states that occur in negative ion mode. In addition, the identification of di-anionic glycans was facilitated by their appearance in the 140 mM NaCl eluent

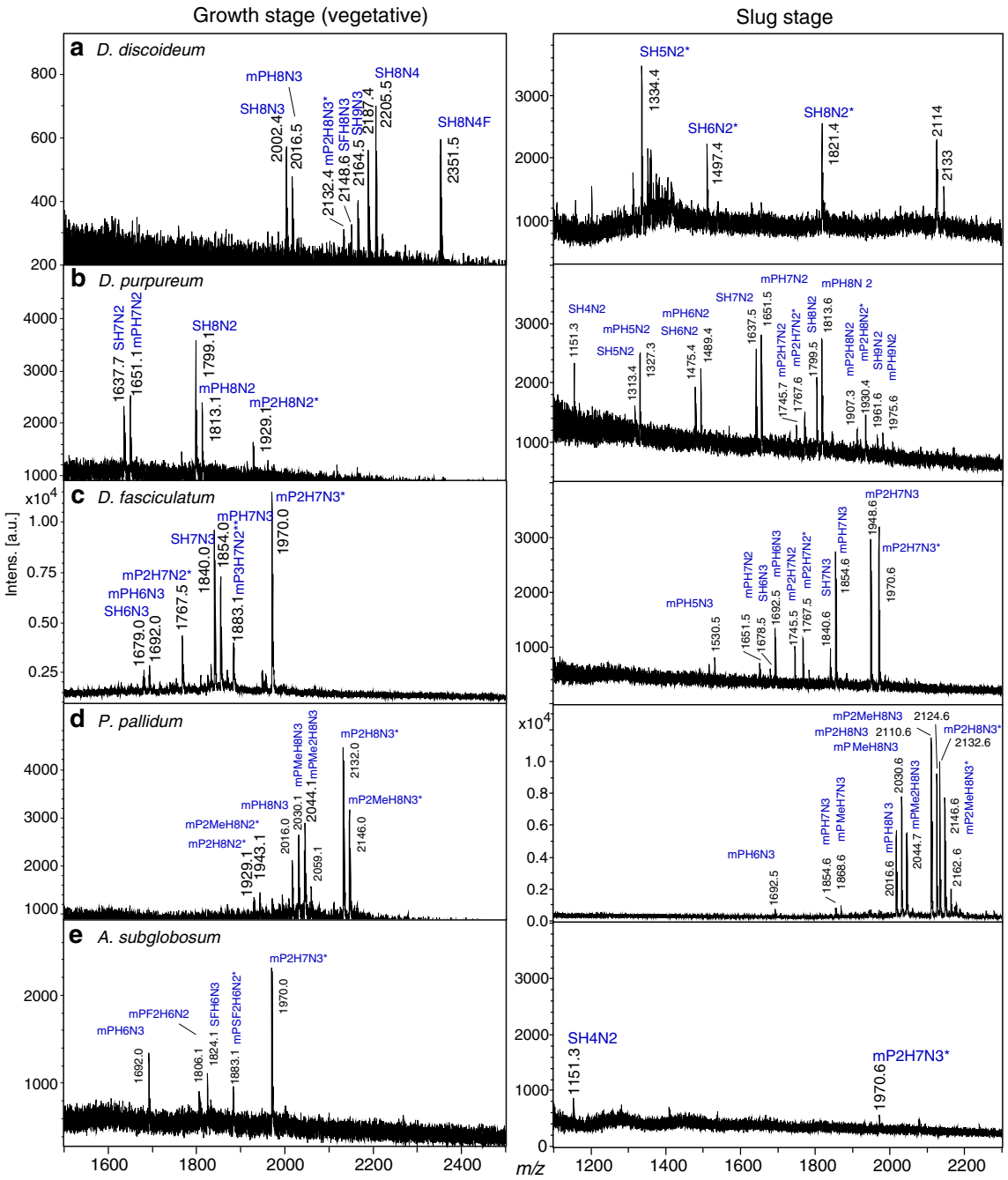

Fig. 7 Anionic glycans. Growth stage cells: left panels; slug stage cells: right panels. N-glycans were enriched by QAE-Sephadex anion exchange chromatography and analyzed by MALDI-TOF-MS in negative ion mode. Ions are $[M–H]^-$, except *=$[M+Na–2H]^-$, as usually seen with glycans containing 2 anionic substituents at least one of which is mP, or **=$[M+2Na–3H]^-$, as seen with glycans containing 3 mP substituents. Representative spectra from different species are shown in panels **a–e**

of the QAE-resin (Fig. S4c). For example, a minor ion appeared at *m/z* 2016.6 in unenriched samples of *Pp* and *As* in positive ion mode (Figs. 6c, e), that was consistent with mP2H7N3 ($[M–2H+3Na]^+$) and SF2H6N3 ($[M–H+2Na]^+$). This corresponded to a major ion that appeared after QAE-enrichment in the 70 mM NaCl fraction, at *m/z* 1970.0 in negative ion mode (Figs. 7c, e), which could be assigned as mP2H7N3 ($[M+Na–2H]^-$) or SF2H6N3 ($[M–H]^-$), and again at 2016.6 in positive ion mode (Fig. S4b). The appearance of this ion in the 140 mM NaCl fraction (Fig. S4c) confirmed its assignment as the di-anionic double methylphosphorylated species, as annotated. The distinction between phosphorylation and sulfation, which introduce similar masses, was facilitated by the tendency of CSMs to esterify their PO_4 groups with CH_3 (Me) groups (mP). Since methylation of neutral N-glycans was not observed in any CSMs except *Pp*, the

presence of the respective masses of Me and PO_4 is assumed to represent methylphosphorylation. In *Pp*, the occurrence of ions with the mass increment of PO_4 or SO_4 in the neutral fraction after permethylation was most consistent with their origin as mP rather than SO_4, because SO_4 groups are not methylated under these conditions. In addition, the putative di-mP *Pp* species tended to ionize as a pair of $[M–H]^-$ and $[M–2H+Na]^-$ ions in negative ion mode (Fig. 7d, right), as observed for di-mP species in *Dp* and *Df*. Thus the anionic species in *Pp* appear to be methylphosphorylated rather than sulfated, and also methylated at separate sites.

As summarized in Figs. 8g and i, mP was found on N-glycans of all species, and sulfation was abundant in all but *Pp* where it was minimal if present at all. N-glycans with up to 2 mP residues were observed, more than a single SO_4 (S) was uncommon, and mixed methylphosphorylated/sulfated N-glycans were observed. The profile of anionic glycans showed negligible overlap between the species. Based on negative ion mode analysis of native glycans, methylphosphorylated and sulfated N-glycans had similar relative abundance, except for *Dd* and *As* where sulfation was modestly more prevalent and *Pp* where it was not detected (Fig. 8i). In positive ion mode analysis of permethylated samples, in which methylphosphorylated glycans are neutral and preferentially observed, methylphosphorylated glycans represented approximately 20 % of the total (Fig. 8g), suggesting that on average, total anionic glycans represent over a third of total N-glycans. The patterns of anionic substitution were not foretold simply by the abundance of underlying backbones. In *Dp*, Man(7–8) glycans were modified with either SO_4 or mP, however $Man_9GlcNAc_2$ and $Glc_3Man_9GlcNAc_2$ glycans were not (Fig. 7b). In *Df*, the predominant H7 species were also sulfated or methylphosphorylated, but in *As* these substitutions were restricted to the H6 species, which were also the main target of fucosylation which in some cases was simultaneous (Figs. 7c, e). In *Pp*, the sum of mP and Me groups did not exceed 3, suggesting that these modifications are mutually exclusive. Since methylphosphorylation occurs on the 6-position of terminal and subterminal Man residues of each arm [5], and methylation evidently occurs at the subterminal Man of each arm (see above), exclusivity may lie at the level of the terminal disaccharide.

Sulfation and methylphosphate changes during development

Anionic glycan changes recapitulated many of the changes observed in neutral glycans of the slug stage. During development *Dd* showed a marked decrease in the relative abundance of methylphosphorylated and sulfated N-glycans (Fig. 8h) consistent with previous reports [17, 36]. The remaining anionic N-glycans are predominantly sulfated, only on N-glycans that lack peripheral GlcNAc residues (Fig. 7a, right panel). Similarly, *As* showed significant decreases in the overall levels of sulfation and methylphosphorylation in slugs. *Dp* maintained similar methylphosphorylation and sulfation and applied them to the more highly trimmed Man structures. *Df* and *Pp* exhibited modestly increased methylphosphorylation, that extended to the more highly trimmed Man structures and at the expense of sulfation in the case of *Df*. *Pp*, which did not extensively trim its Man structures, continued to lack sulfation (Fig. 7d, right panels).

Discussion

Traditional high mannose type N-glycosylation is a global feature across CSM evolution, with no evidence for maturation to traditional paucimannose, hybrid, or complex N-glycans. This feature was also found for another amoebazoan, *Acanthamoeba* [37], and in a modified form in a more distantly related amoebazoan, *Entamoeba* [38], which utilizes a truncated Man_5- rather than Man_9-containing lipid-linked precursor. Also conserved across the CSMs are a peripheral HexNAc residue, α3-core fucosylation, and peripheral sulfation and methylphosphorylation. Remarkably, these modifications are absent from N-glycans of the other characterized amoebazoans *Acanthamoeba* [37] and *Entamoeba* [38]. In contrast, these other amoebazoans diversify their N-glycans in distinctive fashion, by the addition of peripheral Gal in α2-linkage to Man [38], core α6-linked Fuc which can be extended by αMan, peripheral non-methylated phosphomannose, and pentosylation at multiple sites [37]. Therefore the distinctive traits in the CSMs, including the enzymes that apply them and the genes that encode them, were evidently acquired early in their evolution and their retention suggests important CSM specific functions.

Despite these commonalities, the glycomic profiles of the 5 species are remarkably divergent (Figs. 2 and 6). The differences are attributable in part to variations in Man residue trimming, resulting in a different spectrum of backbone structures available for further processing. This is amplified by variations in the number of peripheral HexNAc residues (0–2), core and peripheral Fuc residues (0–3), sulfates (0–2), and/or methylphosphates (0–2). Species-specific modifications contributed further diversity: peripheral Man methylation (0–3) in *Pp*, Glc_3-retention in *Dp*, and apparent lack of fucosylation in *Df* and sulfation in *Pp*. Thus a unique fingerprint of N-glycan types, with limited overlap, is characteristic of the growing cells of each species (summarized in Fig. 8). Mechanisms for controlling these variations, and their potential interdependence, can now be addressed.

The peripheral HexNAc residues of *Dd* are GlcNAc β4-linked to the α6-linked Man (intersecting) and the β4-linked Man (bisecting) [32], and evidence favors an intersecting position for the single peripheral HexNAc of *Pp* N-glycans

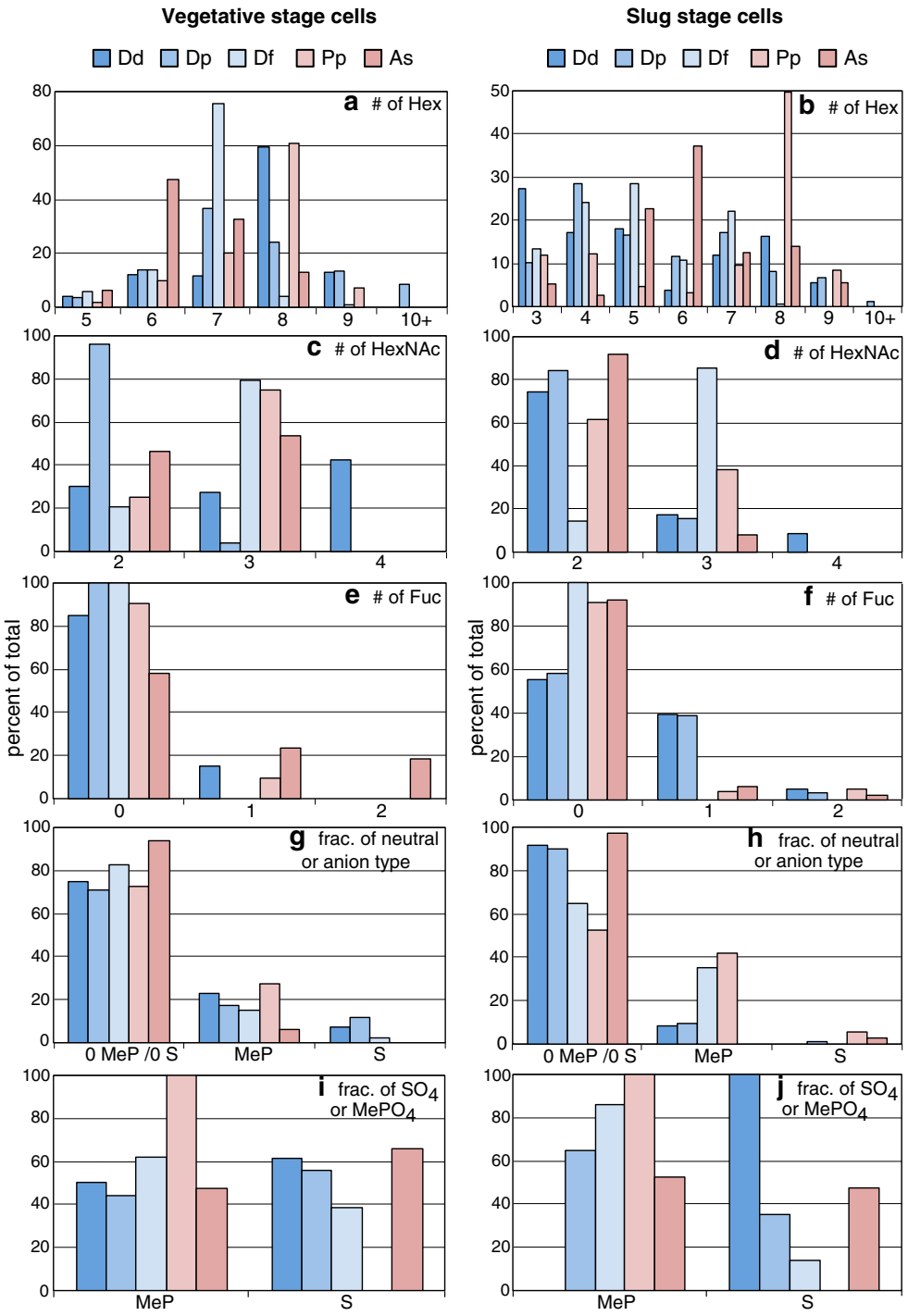

Fig. 8 Quantitation of neutral and anionic N-glycan classes from growing (left column: **a, c, e, g, i**) and developed slug (right column: **b, d, f, h, j**) cells. **a–f**. The abundance of each neutral N-glycan subclass was calculated by dividing the sum of the ion currents of each of its constituents by the summed ion current for all growth stage permethylated neutral N-glycans analyzed in the positive ion mode (data not shown). **g, h**. The relative abundance of anionic glycans was estimated from permethylated native glycans analyzed in positive ion mode. **i, j**. Since sulfated glycans retain their negative charge and are underrepresented by this method, native glycans were analyzed in negative ion mode (where neutral glycans are poorly detected) to facilitate comparison between methylphosphorylated and sulfated glycan levels. Data were averaged from 2 to 4 biological replicates

(Fig. 5d). *Dd* has three tandem genes with distant similarity to the CAZy GT17 family [31], which includes GlcNAcT-III that attaches the bisecting GlcNAc in animals. These are thus candidates for mediating the addition of the bisecting and/or intersecting βGlcNAcs of *Dd*, though unlike the animal enzyme the *Dictyostelium* enzymes do not depend on prior action of GlcNAcT-I and α-mannosidase I. Interestingly, these genes are apparently absent from *Dp*, *Pp* and *As* (not shown), which argues against their role in the addition of their peripheral HexNAc residue. An alternative possibility is that the HexNAc in these other species is a GlcNAc in α4-linkage to the β-Man, as recently reported for the fungus *Coprinus cinerea* [39]. *Dp* and *Df* possess a GT8 family gene related to the α4-GlcNAcT that mediates formation of this linkage in fungi. However, neither was detected in *Pp* and *As* (not shown), leaving the origin and identity of their third HexNAc in need of further investigation. Like the fungal glycans modified with α-GlcNAc, the N-glycans of *Dp* and *Df*

with a peripheral HexNAc are resistant to release by Endo H (Fig. S3), but so also are the N-glycans of the other species with a peripheral β-GlcNAc, under the conditions employed in this study.

Fucosylation is a common modification in each of the species except for *Df*. The great majority of fucosylated N-glycans are inferred to possess a core α3-linked Fuc, as documented previously in *Dd* [7], because fucosylated N-glycans are released by PNGase A but not PNGase F. This conclusion is consistent with expression of the HRP epitope (Fig. 3). Multiply fucosylated species were found in *Dd*, *Pp* and *As*. Previous MS/MS studies indicated a peripheral Man-linkage for additional Fuc residues in *Dd* [6]. Further studies are needed to confirm this for *Pp* and *As*, and to define the positions of these linkages. There are multiple α3FucT-like genes, 10 in *Dd* [31] and 5 *Dp* [3], that might contribute to their assembly. The apparent absence of N-glycan fucosylation in *Df* suggests that its α3FucT-like genes target different glycan types.

Most organisms express anionic N-glycans, and this role is fulfilled by peripheral sulfation and methylphosphorylation in *Dd* [12, 40, 41]. This feature is conserved in the other CSMs (Fig. 7), except for minimal or no sulfation in *Pp* (Fig. 8). Gpt1, the enzyme that mediates the initial transfer of GlcNAc-PO_4 from UDP-GlcNAc to peripheral Man residues of N-glycans in *Dd* [42], is conserved in all the CSM genomes (not shown). However, the genetic bases for removal of the GlcNAc and subsequent methylphosphorylation remain to be determined. Me-PO_4 was not observed in *Acanthamoeba* [37], so the responsible methyltransferase might be mined from a genomic comparison of amoebazoan genes. Since sulfation was also not found in the other amoebazoans, the enzyme(s) that forms the SO_4-Man linkages may be identified by a similar approach.

Methylation is unique to *Pp* N-glycans among the five CSMs examined. Three CH_3 groups per glycan is most frequent (Fig. 5a), and they appear to prefer subterminal Man residues on each arm of the H8N3 backbone (Fig. 5c). Based on the profiles observed, methylation is antagonistic with fucosylation on the same N-glycan, but is tolerant of mP (Figs. 7d, S4). Methylation also occurs in *Acanthamoeba*, where a single moiety was mapped to the Man α3-linked to the core β-Man [37]. CH_3-Man was observed in nematodes [43] and mapped to the 3-O-position of Man in gastropods [44]. The CH_3-linkage of *Pp* remain to be determined.

The terminal Glc_3-moiety of the lipid-linked oligosaccharide precursor is almost universally removed after transfer of the glycan to protein as part of ER quality control of protein folding [45, 46]. As previously described in *Dd*, the other CSMs conform to this principle except for *Dp*, which in this study consistently expressed tri- and mono-glucosylated species during growth (Fig. 4), and tri-, di-, and mono-glucosylated species in the slug (Fig. 6b). While the mono-glucosylated species might reflect activity of the UDP-Glc-dependent αGlcT owing to persistent engagement of the carrier proteins in the calnexin cycle, the tri- and di-Glc species suggest reduced activity of α-glucosidase-I and -II. Since glucosylated N-glycans were not observed in a previous study that analyzed CHAPS-solubilized *Dd* and *Dp* N-glycoproteins [3], these underprocessed species might belong to a protein pool that was not accessed using that approach. Retention of a terminal Glc is common on N-glycans of a cell surface glycoprotein in *Leishmania* species [47].

The N-glycan repertoire of growth stage cells is under dramatic regulation in response to nutritional deprivation in *Dd* [5, 7], and analysis of the slug stage confirms this as a principle for all the CSMs (Figs. 6 and 7). The common theme among all 5 species is increased α-mannosidase trimming of glycans in slugs compared to growing cells, resulting in a reduced average size but still a considerable overlap of structures ranging from H3 to H9 (Fig. 8a, b). Other features, however, diverge. Fucosylation is strongly up- or down-regulated in species-specific fashion. Fucosylation increases in *Dd*, *Dp* and *Pp*, but becomes nearly undetectable in *As*. The peripheral HexNAc residue is selectively and dramatically reduced in *As*, as occurs in *Dd* [9], but does not change in the other species. *Pp* methylation is modestly decreased. Methylphosphorylation, strongly reduced in *Dd* as previously described [5], is modestly decreased in *Dp* but increased in *Df*. The slug N-glycome presumably represents the sum of carryover from growth stage cells and new synthesis in emergent prestalk and prespore cells, and further studies are needed to resolve their relative contributions. It is expected that the slug-unique glycan species are newly synthesized rather than remodeled from prior glycans, given the ongoing general synthesis of new proteins during the developmental program.

The only conserved developmentally regulated N-glycomic change is increased mannose trimming. Studies in *Dd* implicate contributions of both α-mannosidase-I and -II activities [9], whose corresponding inhibitors do not, however, impact the developmental program under laboratory conditions. The finding that the other N-glycomic changes were not shared across the CSMs and that the structures do not converge to a common pattern, suggests that they do not subserve shared general developmental mechanisms such as chemotaxis, cell adhesion, cell sorting, morphogenesis, and cell differentiation. Nevertheless, individual species have distinctive developmental features [24] that might be supported by their glycan differences. For example, *Pp* assembles small lateral fruiting bodies on a larger vertical fruiting body, *Dp* forms an extended stalk, and *As* does not form specialized stalk cells; any of these differences might be supported by specialized glycans.

The N-glycans for this study were derived from whole cells and thus reflect the composition not only of the cell surface glycocalyx but also the internal endomembrane system and

vesicle contents including lysosomal enzymes. Interestingly, recent analysis of a single cell surface *Dd* glycoprotein, gp130, identified the entire spectrum of known *Dd* N-glycans in association with at least one of its 18 N-glycan sites [6]. Assuming that this promiscuity is general across the other CSMs, it is likely that the species differences observed here occur at their cell surfaces and potentially influence interactions with other CSMs, prey, predators and parasites. Different strains and species of CSMs encounter one another in the soil environment, and exhibit avoidance responses at various times before or during development [10, 11], and glycan differences, which are a dominant feature of the glycocalyx, might contribute to intercellular recognition. Some strains of *Dd* exhibit preferential kin association [48] and strain-specific N-glycomic variations might contribute to this process too. Interestingly, a genetic analysis suggests that N-glycosylation and gp130 contribute to differential recognition of gram-negative and gram-positive prey bacteria by *Dd* [12]. *Dd* can be colonized by certain bacteria [49], so glycosylation differences among the CSMs might support evasion from pathogens as proposed in other host-pathogen relationships [50]. Alternatively, differences might be selectively permissive for colonization by commensal bacteria [51]. Generalizing from a concept in innate immunity, the distinctive N-glycan profiles are candidates for microbe-associated molecular patterns that might be recognized by pattern recognition receptors [52]. The comparative N-glycomic analysis reported here will enable future identification of glycogene targets that will permit mutational analyses of the proposed N-glycan roles in these processes.

Acknowledgments This project was partially supported by NIH R01-GM037539 and the OCMG, which received funding from the OUHSC Dept. of Biochemistry & Molecular Biology and the OUHSC VP Office for Research. We are grateful to Jennifer Johnson for her technical assistance, the *Dictyostelium* Stock Center (Northwestern University) and Adam Kuspa (Baylor) for providing cells, and to Christine Scaman (Univ. of British Columbia) for providing yeast α-glucosidase-I.

Conflict of interest None declared.

References

1. Schaap, P.: Evolutionary crossroads in developmental biology: *Dictyostelium discoideum*. Development **138**, 387–396 (2011)
2. Heidel, A.J., Lawal, H.M., Felder, M., Schilde, C., Helps, N.R., Tunggal, B., Rivero, F., John, U., Schleicher, M., Eichinger, L., Platzer, M., Noegel, A.A., Schaap, P., Glöckner, G.: Phylogeny-wide analysis of social amoeba genomes highlights ancient origins for complex intercellular communication. Genome Res. **21**, 1882–1891 (2011)
3. Sucgang, R., Kuo, A., Tian, X., Salerno, W., Parikh, A., Feasley, C.L., Dalin, E., Tu, H., Huang, E., Barry, K., Lindquist, E., Shapiro, H., Bruce, D., Schmutz, J., Salamov, A., Fey, P., Gaudet, P., Anjard, C., Babu, M.M., Basu, S., Bushmanova, Y., van der Wel, H., Katoh-Kurasawa, M., Dinh, C., Coutinho, P.M., Saito, T., Elias, M., Schaap, P., Kay, R.R., Henrissat, B., Eichinger, L., Rivero, F., Putnam, N.H., West, C.M., Loomis, W.F., Chisholm, R.L., Shaulsky, G., Strassmann, J.E., Queller, D.C., Kuspa, A., Grigoriev, I.V.: Comparative genomics of the social amoebae *Dictyostelium discoideum* and *Dictyostelium purpureum*. Genome Biol. **12**, R20 (2011)
4. Dykstra, M.J., Aldrich, H.C.: Successful demonstration of an elusive cell coat in amebae. J. Protozool. **25**, 38–41 (1978)
5. Freeze, H.H.: *Dictyostelium discoideum* glycoproteins: using a model system for organismic glycobiology. In: Glycoproteins II. Eds.: Montreuil, J.F.G. Vliegenthart and H. Schachter, Elsevier Science B.V. pp. 89–121 (1997)
6. Feasley, C.L., Johnson, J.M., West, C.M., Chia, C.P.: Glycopeptidome of a heavily N-glycosylated cell surface glycoprotein of *Dictyostelium* implicated in cell adhesion. J. Proteome Res. **9**, 3495–3510 (2010)
7. Schiller, B., Hykollari, A., Voglmeir, J., Pöltl, G., Hummel, K., Razzazi-Fazeli, E., Geyer, R., Wilson, I.B.: Development of *Dictyostelium discoideum* is associated with alteration of fucosylated N-glycan structures. Biochem. J. **423**, 41–52 (2009)
8. Hykollari, A., Balog, C.I., Rendić, D., Braulke, T., Wilson, I.B., Paschinger, K.: Mass spectrometric analysis of neutral and anionic N-glycans from a *Dictyostelium discoideum* model for human congenital disorder of glycosylation CDG IL. J. Proteome Res. **12**, 1173–1187 (2013)
9. Sharkey, D.J., Kornfeld, R.: Developmental regulation of asparagine linked oligosaccharide synthesis in *Dictyostelium discoideum*. J. Biol. Chem. **266**, 18485–18497 (1991)
10. Nicol, A., Garrod, D.R.: Mutual cohesion and cell sorting-out among four species of cellular slime moulds. J. Cell Sci. **32**, 377–387 (1978)
11. Sathe, S., Khetan, N., Nanjundiah, V.: Interspecies and intraspecies interactions in social amoebae. J. Evol. Biol. **27**, 349–362 (2014)
12. Nasser, W., Santhanam, B., Miranda, E.R., Parikh, A., Juneja, K., Rot, G., Dinh, C., Chen, R., Zupan, B., Shaulsky, G., Kuspa, A.: Bacterial discrimination by dictyostelid amoebae reveals the complexity of ancient interspecies interactions. Curr. Biol. **23**, 862–872 (2013)
13. Champion, A., Griffiths, K., Gooley, A.A., Gonzalez, B.Y., Gritzali, M., West, C.M., Williams, K.L.: Immunochemical, genetic and morphological comparison of fucosylation mutants of *Dictyostelium discoideum*. Microbiology **141**, 785–797 (1995)
14. Houle, J., Balthazar, J., West, C.M.: A glycosylation mutation affects cell fate in chimeras of *Dictyostelium discoideum*. Proc. Natl. Acad. Sci. U. S. A. **86**, 3679–3683 (1989)
15. West, C.M.: Comparative analysis of spore coat formation, structure, and function in *Dictyostelium*. Int. Rev. Cytol. **222**, 237–293 (2003)
16. Wang, F., Metcalf, T., van der Wel, H., West, C.M.: Initiation of mucin-type O-glycosylation in *Dictyostelium* is homologous to the corresponding step in animals and is important for spore coat function. J. Biol. Chem. **278**, 51395–51407 (2003)
17. Bush, J.M., Ebert, D.L., Cardelli, J.A.: Alterations to N-linked oligosaccharides which affect intracellular transport rates and regulated secretion but not sorting of lysosomal acid phosphatase in *Dictyostelium discoideum*. Arch. Biochem. Biophys. **283**, 158–166 (1990)
18. Souza, G.M., Mehta, D.P., Lammertz, M., Rodriguez-Paris, J., Wu, R., Cardelli, J.A., Freeze, H.H.: *Dictyostelium* lysosomal proteins with different sugar modifications sort to functionally distinct compartments. J. Cell Sci. **110**, 2239–2248 (1997)
19. West, C.M., Wang, Z.A., van der Wel, H.: A cytoplasmic prolyl hydroxylation and glycosylation pathway modifies Skp1 and regulates O_2-dependent development in *Dictyostelium*. Biochim. Biophys. Acta. **1800**, 160–171 (2010)

20. Zhang, D., van der Wel, H., Johnson, J.M., West, C.M.: Skp1 prolyl 4-hydroxylase of *Dictyostelium* mediates glycosylation-independent and -dependent responses to O_2 without affecting Skp1 stability. J. Biol. Chem. **287**, 2006–2016 (2012)
21. Feasley, C.L., Hykollari, A., Paschinger, K., Wilson, I.B., West, C.M.: N-glycomic and -glycoproteomic studies in the social amoebae. Meth. Mol. Biol. **983**, 205–229 (2013)
22. Hykollari, A., Dragosits, M., Rendić, D., Wilson, I.B., Paschinger, K.: N-glycomic profiling of a glucosidase II mutant of *Dictyostelium discoideum* by "off-line" liquid chromatography and mass spectrometry. Electrophoresis **35**, 2116–2129 (2014)
23. Basu, S., Fey, P., Pandit, Y., Dodson, R., Kibbe, W.A., Chisholm, R.L.: DictyBase 2013: integrating multiple Dictyostelid species. Nucleic Acids Res. **41**(Database issue), D676–D683 (2013)
24. Romeralo, M., Skiba, A., Gonzalez-Voyer, A., Schilde, C., Lawal, H., Kedziora, S., Cavender, J.C., Glöckner, G., Urushihara, H., Schaap, P.: Analysis of phenotypic evolution in Dictyostelia highlights developmental plasticity as a likely consequence of colonial multicellularity. Proc. Biol. Sci. **280**, 20130976 (2013)
25. Fey, P., Kowal, A.S., Gaudet, P., Pilcher, K.E., Chisholm, R.L.: Protocols for growth and development of *Dictyostelium discoideum*. Nat. Protoc. **2**, 1307–1316 (2007)
26. Kang, P., Mechref, Y., Novotny, M.V.: High-throughput solid-phase permethylation of glycans prior to mass spectrometry. Rapid Commun. Mass Spectrom. **22**, 721–734 (2008)
27. Khoo, K.H., Yu, S.Y.: Mass spectrometric analysis of sulfated N- and O-glycans. Meth. Enzymol. **478**, 3–26 (2010)
28. Damerell, D., Ceroni, A., Maass, K., Ranzinger, R., Dell, A., Haslam, S.M.: The GlycanBuilder and GlycoWorkbench glycoinformatics tools: updates and new developments. Biol. Chem. **393**, 1357–1362 (2012)
29. Barker, M.K., Wilkinson, B.L., Faridmoayer, A., Scaman, C.H., Fairbanks, A.J., Rose, D.R.: Production and crystallization of processing α-glucosidase I: *Pichia pastoris* expression and a two-step purification toward structural determination. Protein Expr. Purif. **79**, 96–101 (2011)
30. Dhanawansa, R., Faridamoayer, A., van der Merwe, G., Li, Y.X., Scaman, C.H.: Overexpression, purification, and partial characterization of *Sacchromyces cerevisiae* processing alpha-glucosidase I. Glycobiology **12**, 229–234 (2002)
31. West, C.M., van der Wel, H., Coutinho, P.M., Henrissat, B.: Glycosyltransferase genomics in *Dictyostelium discoideum*. In: *Dictyostelium* Genomics. Eds.: Loomis, W.F., and Kuspa, A. (Horizon Scientific Press, Norfolk, UK) pp. 235–264 (2005)
32. Couso, R., van Halbeek, H., Reinhold, V., Kornfeld, S.: The high mannose oligosaccharides of *Dictyostelium discoideum* glycoproteins contain a novel intersecting N-acetylglucosamine residue. J. Biol. Chem. **262**, 4521–4527 (1987)
33. Sharkey, D.J., Kornfeld, R.: Identification of an N-acetylglucosaminyltransferase in *Dictyostelium discoideum* that transfers an intersecting N-acetyl glucosamine residue to high mannose oligosaccharides. J. Biol. Chem. **264**, 10411–10419 (1989)
34. Srikrishna, G., Wang, L., Freeze, H.H.: Fucose-beta-1-P-Ser is a new type of glycosylation: using antibodies to identify a novel structure in *Dictyostelium discoideum* and study multiple types of fucosylation during growth and development. Glycobiology **8**, 799–811 (1998)
35. Nakagawa, M., Tojo, H., Fujii, S.: A glycan of Psi-factor from *Dictyostelium discoideum* contains a bisecting-GlcNAc, an intersecting-GlcNAc, and a core α-1,6-fucose. Biosci. Biotechnol. Biochem. **75**, 1964–1970 (2011)
36. Knecht, D.A., Dimond, R.L.: Lysosomal enzymes possess a common antigenic determinant in the cellular slime mold, *Dictyostelium discoideum*. J. Biol. Chem. **256**, 3564–3575 (1981)
37. Schiller, B., Makrypidi, G., Razzazi-Fazeli, E., Paschinger, K., Walochnik, J., Wilson, I.B.: Exploring the unique N-glycome of the opportunistic human pathogen *Acanthamoeba*. J. Biol. Chem. **287**, 43191–43204 (2012)
38. Magnelli, P., Cipollo, J.F., Ratner, D.M., Cui, J., Kelleher, D., Gilmore, R., Costello, C.E., Robbins, P.W., Samuelson, J.: Unique *As*n-linked oligosaccharides of the human pathogen *Entamoeba histolytica*. J. Biol. Chem. **283**, 18355–18364 (2008)
39. Buser, R., Lazar, Z., Käser, S., Künzler, M., Aebi, M.: Identification, characterization, and biosynthesis of a novel N-glycan modification in the fruiting body of the basidiomycete *Coprinopsis cinerea*. J. Biol. Chem. **285**, 10715–10723 (2010)
40. Freeze, H.H., Bush, J.M., Cardelli, J.: Biochemical and genetic analysis of an antigenic determinant found on N-linked oligosaccharides in *Dictyostelium*. Dev. Genet. **11**, 463–472 (1990)
41. Cardelli, J.A., Bush, J.M., Ebert, D., Freeze, H.H.: Sulfated N-linked oligosaccharides affect secretion but are not essential for the transport, proteolytic processing, and sorting of lysosomal enzymes in *Dictyostelium* discoideum. J. Biol. Chem. **265**, 8847–8853 (1990)
42. Qian, Y., West, C.M., Kornfeld, S.: UDP-GlcNAc:Glycoprotein N-acetylglucosamine-1-phosphotransferase mediates the initial step in the formation of the methylphosphomannosyl residues on the high mannose oligosaccharides of *Dictyostelium discoideum* glycoproteins. Biochem. Biophys. Res. Commun. **393**, 678–681 (2011)
43. Cipollo, J.F., Awad, A.M., Costello, C.E., Hirschberg, C.B.: N-Glycans of *Caenorhabditis elegans* are specific to developmental stages. J. Biol. Chem. **280**, 26063–26072 (2005)
44. Gutternigg, M., Bürgmayr, S., Pöltl, G., Rudolf, J., Staudacher, E.: Neutral N-glycan patterns of the gastropods *Limax maximus*, *Cepaea hortensis*, *Planorbarius corneus,* Arianta arbustorum and Achatina fulica. Glycoconj. J. **24**, 475–489 (2007)
45. Banerjee, S., Vishwanath, P., Cui, J., Kelleher, D.J., Gilmore, R., Robbins, P.W., Samuelson, J.: The evolution of N-glycan-dependent endoplasmic reticulum quality control factors for glycoprotein folding and degradation. Proc. Natl. Acad. Sci. U. S. A. **104**, 11676–11681 (2007)
46. Schiller, B., Hykollari, A., Yan, S., Paschinger, K., Wilson, I.B.: Complicated N-linked glycans in simple organisms. Biol. Chem. **393**, 661–673 (2012)
47. Funk, V.A., Thomas-Oates, J.E., Kielland, S.L., Bates, P.A., Olafson, R.W.: A unique, terminally glucosylated oligosaccharide is a common feature on *Leishmania* cell surfaces. Mol. Biochem. Parasitol. **84**, 33–48 (1997)
48. Hirose, S., Benabentos, R., Ho, H.I., Kuspa, A., Shaulsky, G.: Self-recognition in social amoebae is mediated by allelic pairs of tiger genes. Science **333**, 467–470 (2011)
49. Clarke, M.: Recent insights into host-pathogen interactions from *Dictyostelium*. Cell. Microbiol. **12**, 283–291 (2010)
50. Varki, A.: Nothing in glycobiology makes sense, except in the light of evolution. Cell **126**, 841–845 (2006)
51. Brock, D.A., Read, S., Bozhchenko, A., Queller, D.C., Strassmann, J.E.: Social amoeba farmers carry defensive symbionts to protect and privatize their crops. Nat. Commun. **4**, 2385 (2013)
52. Erbs, G., Newman, M.A.: The role of lipopolysaccharide and peptidoglycan, two glycosylated bacterial microbe-associated molecular patterns (MAMPs), in plant innate immunity. Mol. Plant Pathol. **13**, 95–104 (2012)